ELSEVIER

Ultramicroscopy 82 (2000) 79–83

ultramicroscopy

www.elsevier.nl/locate/ultramic

Amplitude curves and operating regimes in dynamic atomic force microscopy

Ricardo García*, Alvaro San Paulo

Instituto de Microelectrónica de Madrid, CSIC, Isaac Newton 8, 28760 Tres Cantos, Madrid, Spain

Received 31 May 1999; received in revised form 2 September 1999

Abstract

The experimental dependence of the amplitude on the average tip–sample distance has been studied to understand the operation of an atomic force microscope with an amplitude modulation feedback. The amplitude curves can be classified in three major groups according to the existence or not of a local maximum and how the maximum is reached (steplike discontinuities vs. smooth transitions). A model describing the cantilever motion as a forced nonlinear oscillator allows to associate the features observed in the amplitude curves with the tip-sample interaction force. The model also allows to define two elemental tip–sample interaction regimes, attractive and repulsive. The presence of a local maximum in the amplitude curves is related to a transition between the attractive and the repulsive regime.

1. Introduction

Dynamic atomic force microscopy (AFM) methods are widely used for imaging and manipulation of materials in air [1–4], liquid environments [5–7] or ultra high vacuum [8]. At least two factors explain its extensive use, (i) the frictional forces existing between tip and sample are greatly reduced with respect to contact AFM and (ii) the normal force exerted on the sample can also be controlled in dynamic AFM.

In air or liquid environments, the standard dynamic AFM operation uses the oscillation amplitude as the feedback parameter. Dynamic AFM with an amplitude modulation feedback is usually known as tapping-mode or intermittent contact AFM. Tapping-mode AFM has been defined as a high-amplitude dynamic mode where the cantilever-tip ensemble is oscillated at a frequency close to its resonance. The sample is imaged while the feedback adjusts the tip–sample separation to keep the oscillation amplitude at a fixed value. Its name suggests that repulsive forces arising from the tip–sample mechanical contact are responsible for the amplitude reduction. However this is largely misleading. In fact, the feedback mechanism is unable to establish whether the amplitude reduction is the result of attractive, repulsive or a combination of both interactions. Several authors have already emphasized the influence of attractive forces in controlling the amplitude reduction [9–15].

The study of the dependence of the amplitude on the average tip–sample distance is of fundamental importance to understand the operation of a

* Corresponding author. Fax: + 34-91806-0701.
E-mail address: rgarcia@imm.cnm.csic.es (R. García)

0304-3991/00/$ - see front matter
PII: S0304-3991(99)00132-1

dynamic atomic force microscope. In a previous contribution [13] we have developed a model to describe the cantilever motion under the action of long- and short-range tip–sample forces. There, we have found two elemental interaction regimes in dynamic AFM, *attractive and repulsive regimes*, respectively. In the attractive regime, the tip–sample force averaged in one oscillation is negative while in the repulsive regime, the average force is positive. With this definition both regimes may involve long-range attractive and short-range repulsive forces. This definition of operating regimes is more general and allows a clearer description of the cantilever motion than the definition used by Anczykowski et al. [9] and Kühle et al. [10,11], where the attractive regime involved exclusively long-range attractive forces. In this contribution we study the signature of those regimes in the experimental amplitude curves. We also provide a general scheme to identify, classify and understand the features observed in the experimental curves. We believe that the proposed identification could be very useful to improve the imaging contrast in dynamic AFM.

2. Experimental and simulation details

Freshly cleaved mica and a semiconductor (2 monolayers of InAs deposited on GaAs) have been the samples where the dependence of amplitude on tip–sample separation (z-piezo displacement) were studied. The experiments have been performed with a nanoscope III multimode scanning probe microscope (Digital Instruments). All measurements have been made in air at a relative humidity of 35%. Commercial silicon cantilevers with a spring constant k of 40 N/m, nominal tip radius of about 20 nm, resonance frequency f_0 of 325 kHz and quality factor Q of 400 were used. Each cantilever was excited at its free resonance frequency.

The dynamic response of the cantilever-tip ensemble driven by an external and sinusoidal signal has been simulated by a point mass spring under the influence of an external field [9,16–19]. The dominant contributions considered in the equation of motion of the cantilever are its elastic response, the hydrodynamic damping with the medium, the tip–sample interaction and the excitation force. The resulting nonlinear, second-order differential equation is as follows:

$$m\frac{\mathrm{d}z^2}{\mathrm{d}^2t} = -k_c z - \frac{m\omega_0}{Q}\frac{\mathrm{d}z}{\mathrm{d}t} + F_{ts} + F_0\cos\omega t, \quad (1)$$

where F_0 and $\omega(\omega = 2\pi f)$ are the amplitude and angular frequency of the driving force, respectively, Q, ω_0 and k_c are the quality factor, angular resonance frequency and spring constant of the free cantilever, respectively. F_{ts} denotes the tip–sample interaction. Long-range attractive forces are derived from the van der Waals interaction. Adhesion, short-range repulsive forces and sample deformation are modeled by using the DMT contact mechanics. A standard fourth-order Runge–Kutta algorithm has been used to solve Eq. (1). Specific details above the parameters used in the simulations can be found in Ref. [13].

3. Amplitude curves

Amplitude versus z-piezo displacement curves, amplitude curves, are the key elements to describe the operating regimes in dynamic AFM with an amplitude modulation feedback. After performing thousands of experiments with the dynamic AFM excited at the free resonance frequency, we have found that the majority of the experimental amplitude curves could be ascribed to one of the three groups shown in Fig. 1.

Fig. 1a shows an amplitude curve obtained on mica for a cantilever with $A_0 = 16$ nm and $f = f_0 = 326$ kHz. At large separations the amplitude is insensitive to tip–sample distance variations. This is followed by a region where the amplitude decreases almost linearly with decreasing the average tip–sample separation, and finally the oscillation amplitude is zero. On the other hand, the amplitude curves shown in Figs. 1b and c are characterized by the presence of a local maximum. The presence of a maximum is indicative of a competition between different interaction regimes. The transition toward the maximum can be steplike (Fig. 1b) or continuous (Fig. 1c). Examples of steplike transitions have

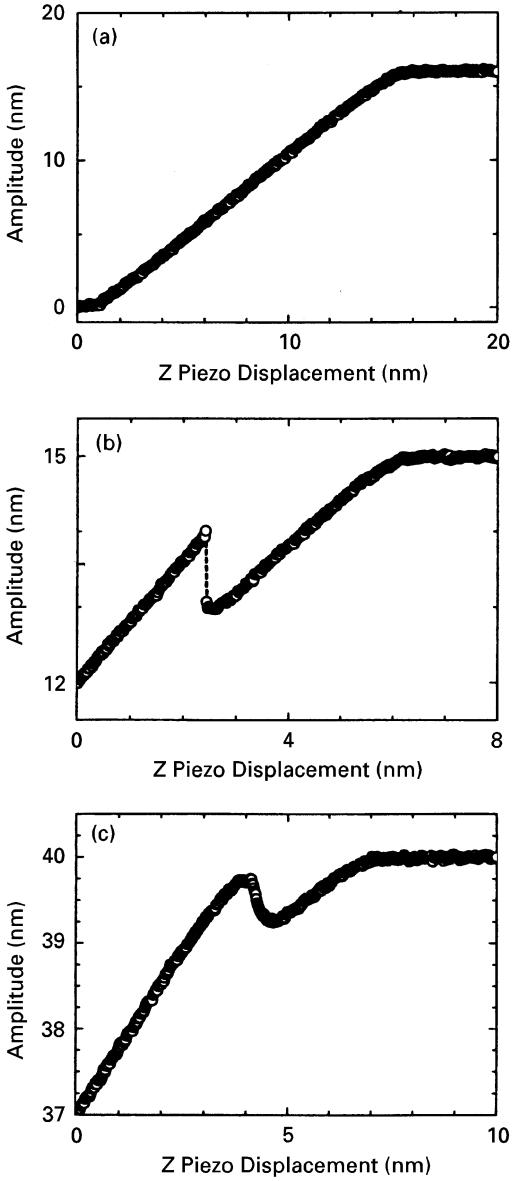

Fig. 1. Experimental amplitude versus z-piezo displacement curves for mica (a) and InAs/GaAs (b and c). Each curve is representative of the three dominant types of amplitude curves. The free amplitude was 16 nm (a) 15 nm (b) and 40 nm (c).

also been reported by Anzcykowski et al. [9] and Kühle et al. [10,11] on SiO_x. Smooth transitions have been observed on polymer samples by Tamayo and García [20] and Chen et al. [21].

To understand the factors controlling the amplitude reduction and to explain the origin of the peaks observed in Figs. 1b and c, we have calculated the amplitude curves for a cantilever with $k = 40$ N/m, $R = 20$ nm, $Q = 400, f = f_0 = 325$ kHz, $E = 130$ GPa and for a sample with a surface energy of 30 mJ/m^2, Hamacker constant of 6.2×10^{-20} J and $E = 1$ GPa. The simulations have been performed for three values of the free amplitude, $A_0 = 6$, 10 and 50 nm respectively. For each value of A_0, the model allows to calculate the amplitude, phase shift, contact time and force as a function of tip–sample separation and time. In addition to the amplitude curves, in Fig. 2 the corresponding average force and contact time experienced by the tip are also plotted. The contact time is defined as the time per oscillation that the tip is in mechanical contact with the sample. The force is averaged over an oscillation period.

Fig. 2a shows a case where the amplitude decreases monotonously with tip–sample separation. These amplitude curves are called type I curves. The examination of the average force and contact time curves indicates that the reduction of the amplitude for type I curves (Fig. 2a) is associated with the exclusive participation of long-range attractive forces. The average force is negative and its absolute value increases as the distance is decreased (Fig. 2d).

When the free amplitude is increased, the calculations also reproduce the peaks observed in the amplitude curves. For $A_0 = 10$ nm, the curve shows a steplike discontinuous transition (type II). The average force profile (Fig. 2e) indicates that the discontinuity marks the transition between an initial region where the amplitude is reduced by the action of long-range attractive forces (the average force is negative and the contact time is equal to zero) to another region where the amplitude reduction is dominated by short-range repulsive forces (the average force is positive with a finite contact time).

The presence of a smooth transition for large amplitudes ($A_0 = 50$ nm) can also be explained by the interplay existing between long-range attractive and short-range repulsive forces (type III). In Fig. 2c the amplitude curve shows both a (local) minimum and a maximum. Initially long-range

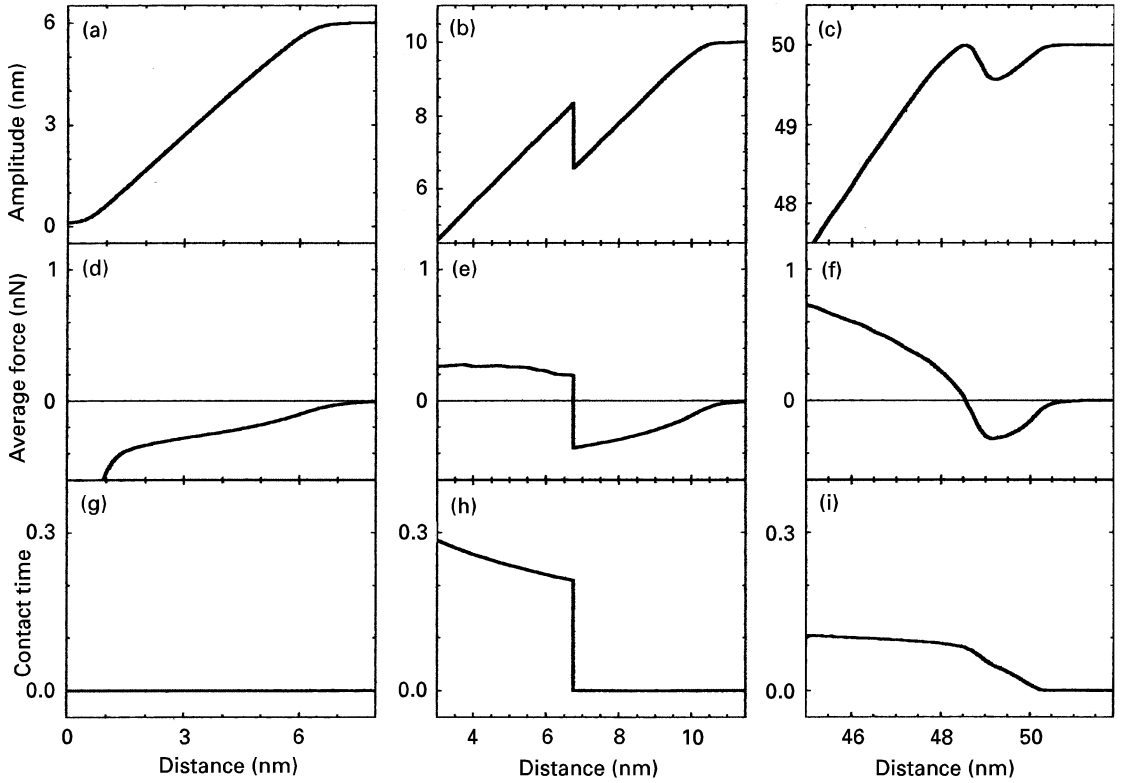

Fig. 2. Theoretical amplitude, average force and contact time curves as a function of the mean tip–sample distance for three different free amplitudes, 6 nm (a, d and g), 10 nm (b, e and h) and 50 nm (c, f and i). The contact time is normalized to the oscillation period.

attractive forces are the dominant interaction controlling the cantilever motion. The average force is negative, however, the contact time (Fig. 2i) has a nonzero value. This means that the amplitude reduction in that region also involves short-range repulsive forces. This result suggested us that a general classification of operating regimes in dynamic AFM should consider the attractive regime also compatible with the existence of tip–sample intermittent contact at one end of the oscillation. When the short-range repulsive forces match the value of the attractive force a local maximum in amplitude is reached (the average force is equal to zero). From then on the amplitude decreases monotonously and short-range repulsive forces dominate the amplitude reduction.

The simulations have reproduced the features observed in the experimental curves, as well as their dependence on the free amplitude (Figs. 1b and c). This supports the interpretation of the peaks obtained in the experimental curves as different transitions between the attractive and repulsive interaction regimes.

There are four relevant observations. First, for a given material, the type of amplitude curves depends on the free amplitude and tip–sample interaction. For example, with InAs/GaAs samples and silicon tips it was hard to find amplitude curves of type I. Second, an amplitude modulation feedback cannot distinguish between an attractive or repulsive interaction regime. For instance, for a set point amplitude $A_{sp} = 13.5$ nm (Fig. 1b) the feedback could choose either a z-piezo diplacement of 1.5 or 3.5 nm to find the set point amplitude. In one case the regime would be repulsive while in the other attractive. Third, a curve with a smooth transition

has a region with a negative slope. This means that an AFM with positive amplitude feedback would produce severe instabilities in that region. Four, in general the attractive regime involves smaller (repulsive) forces than the repulsive interaction regime. To prevent or minimize sample deformation with compliant samples, the use of the attractive regime is recommended.

The above results emphasize the importance of knowing the interaction regime before imaging. As a consequence it is advisable to record an amplitude curve before starting the measurements. Phase-shift curves also reflect the transitions between regimes [13]. They could provide an alternative method to determine the operating regime.

4. Conclusions

Amplitude versus tip–sample distance curves obtained by dynamic AFM have been classified in three major groups. In the first group the amplitude is exclusively controlled by long-range attractive forces. The second and the third groups are characterized by the presence of a local maximum. The maximum reflects the competition between long-range attractive and short-range repulsive forces to control the cantilever dynamics. For type II curves, the maximum is reached through a steplike discontinuity while type III curves show a smooth transition. The comparison between experiments and simulations allows to define two interaction regimes in dynamic AFM, attractive and repulsive. It is important to bear in mind that in some cases, the attractive regime may imply tip–sample intermittent contact, i.e., long-range attractive and short-range repulsive forces controlling the cantilever dynamics. The transition between attractive and repulsive interaction regimes may be abrupt or smooth depending on the free amplitude and sample properties. In general, the attractive regime should be the regime of choice to image compliant samples because tip–sample forces are usually smaller than in the repulsive regime.

Acknowledgements

The semiconductor samples have been gratefully provided by Luisa González and Jorge García. This work has been supported by the European Commission, BICEPS, BIO4-CT-2112.

References

[1] Y. Martin, C.C. Williams, H.K. Wickramasinghe, J. Appl. Phys. 61 (1987) 4723.
[2] R. García, M. Calleja, F. Pérez-Murano, Appl. Phys. Lett. 72 (1998) 2295.
[3] C. Margeat, Le Grimelle, C.A. Royer, Biophys. J. 75 (1998) 2712.
[4] G. Bar, Y. Thomann, M.-H. Whangbo, Langmuir 14 (1998) 1219.
[5] P.K. Hansma, J.P. Cleveland, M. Radmacher, D.A. Walters, P.E. Hillner, M. Bezanilla, M. Fritz, D. Vie, H.G. Hansma, C.B. Prater, J. Massie, L. Fukunaga, J. Gurley, V. Elings, Appl. Phys. Lett. 64 (1994) 1738.
[6] F. Ohnesorge, Surf. Interface Anal. 27 (1999) 379.
[7] M. Lantz, Y.Z. Liu, X.D. Cui, H. Tokumoto, S.M. Lindsay, Surf. Interface Anal. 27 (1999) 354.
[8] F.J. Giessibl, Science 267 (1995) 68.
[9] B. Anczykowski, D. Krüger, H. Fuchs, Phys. Rev. B 53 (1996) 15485.
[10] A. Kuhle, A.H. Sorensen, J.J. Bohr, J. Appl. Phys. 81 (1997) 6562.
[11] A. Kuhle, A.H. Sorensen, J.J. Bohr, Appl. Phys. A 66 (1998) S329.
[12] G. Haugstad, R. Jones, Ultramicroscopy 76 (1999) 77.
[13] R. García, A. San Paulo, Phys. Rev. B 60 (1999) 4961.
[14] J. Colchero, private communication.
[15] R. Boisgard, D. Michel, J.P. Aimé, Surf. Sci. 401 (1998) 199.
[16] D. Sarid, T.G. Rushell, R.K. Workman, D. Chen, J. Vac. Sci. Technol. B 14 (1996) 864.
[17] J. Tamayo, R. García, Langmuir 12 (1996) 4430.
[18] N.A. Burham, O.P. Behrend, F. Ouveley, G. Gremaud, P.-J. Gallo, D. Gordon, E. Dupas, A.J. Kulik, H.M. Pollock, G.A.D. Briggs, Nanotechnology 8 (1997) 67.
[19] N.A. Burham, O.P. Behrend, F. Ouveley, G. Gremaud, P.-J. Gallo, D. Gordon, E. Dupas, A.J. Kulik, H.M. Pollock, G.A.D. Briggs, Appl. Phys. B 66 (1998) S219.
[20] J. Tamayo, R. García, Appl. Phys. Lett. 71 (1997) 2394.
[21] X. Chen, M.C. Davies, C.J. Roberts, S.J.B. Tendler, P.M. Williams, J. Davies, A.C. Dawkes, J.C. Edwards, Ultramicroscopy 75 (1998) 171.